https://doi.org/10.15407/ufm.25.04.708

**M.A. LATYPOVA*, B.B. MAKHMUTOV, and A.S. YERZHANOV**

Karaganda Industrial University,
30 Republic Ave., 101400 Temirtau, Kazakhstan

* m.latypova@tttu.edu.kz

# LAYERED METAL COMPOSITES AS A PROMISING CLASS OF MODERN MATERIALS

The intensive development of the transport, chemical, atomic power engineering, shipbuilding, and aerospace engineering necessitates the creation of new materials with a unique set of physical-mechanical and functional properties. Such materials include an extensive group of layered metal composite materials based on dissimilar and heterogeneous metals and alloys, which, due to the presence of laminated and sandwich structures, allow to obtain a complex of difficult-to-combine properties: high strength, ductility, toughness at low-climatic and cryogenic temperatures, wear resistance, thermal and electrical conductivities. One of the current directions of modern materials science is the development of layered metal composite materials for multifunctional purposes with layers of consolidated mixtures of Al powders and reinforcing particles $Al_2O_3$, SiC, and $B_4C$, which can be used for the fabrication of products and structures with specified tribological and thermophysical characteristics, high ballistic resistance, as well as for the manufacturing of radiation protective elements of the nuclear or space engineering.

**Keywords:** layered materials, composite materials, structure, properties, production methods.

## 1. Introduction

The development of critical industries of the country, such as aircraft and mechanical engineering, space industry, and nuclear power engineering, requires new materials with improved functional properties, as well as technologies for obtaining such materials [1–10]. Laminated composite materials are one of such materials.

Citation: M.A. Latypova, B.B. Makhmutov, and A.S. Yerzhanov, Layered Metal Composites as a Promising Class of Modern Materials, *Progress in Physics of Metals*, **25**, No. 4: 708–735 (2024)

Layered composite materials are a crucial class of composites with an extensive range and a unique combination of valuable properties such as high strength, corrosion resistance, manufacturability, electrical and thermal conductivity, heat resistance, wear resistance, low density, and increased hardness. Layered composites, in some cases, even have exceptional physical and mechanical properties when the thickness of individual layers reaches micro- and nanoscale values.

Layered metal composite materials (LMCM) are part of an extensive class of modern composite materials on a metallic and non-metallic basis, which can be classified according to such characteristics as the type and nature of the matrix (metals, alloys, ceramics, polymers, fibre-glass) and filler (layers, fibres, filamentous crystals, dispersed particles), geometry and the layout of the filler in the matrix, the hardening mechanisms, as well as the production methods [11–15]. The author of the work [15] divides all composite materials into matrix and layered composites.

As believed, the layers in the LMCM, by their functional purpose, are divided into basic and cladding. The main layer is responsible for the structural strength of the composite, and the cladding layers give the LMCM a higher level of plasticity or provide it with functional properties. Layered hybrid composites, which have two or more different reinforcing components in their composition, are more complex in terms of the architecture of LMCM [16]. An example of such a material is LMCM, in which layers of metallic materials (aluminium, titanium, *etc*.) alternate with layers of polymer composite materials. The development in the field of layered hybrid composites is aluminium–fiberglass SIAL. A foreign analogue of this material is GLARE [17], consisting of alternating layers of aluminium foil and continuously oriented grids of high-strength glass fibres impregnated with an epoxy resin-based adhesive.

In recent years, metal matrix composites (MMC) and, in particular, aluminium matrix composites reinforced with particles of aluminium oxides, silicon, and boron carbides have become widespread [15, 18, 19]. Based on these materials, laminated composites consisting of ceramic interlayers located on both the outer and inner parts of the layered material are proposed [20].

The most widely used in industry is LMCM consisting of a set of alternating different metals in the form of sheet, plate, and foil materials rigidly interconnected over the entire surface.

The advantages of LMCM over traditional metal materials include increased endurance limit and resistance to cyclic and dynamic loads due to the inhibitory effect of interlayer boundaries on crack development. Layered composites obtained at the macro level (macrolaminates) with various types of matrix and filler are effectively used in such industries as transport and energy engineering, shipbuilding, and aerospace engineering as structural, corrosion-resistant, ballistic, superconducting and radiation-

protective materials [15, 18, 19]. Conductor and contact microcomposites (of steel–copper, steel–aluminium, and copper–aluminium) are widely used in electrical engineering and instrumentation. Composite pipes and sheets made of aluminium and its alloys obtained by explosion welding [20] are used in fasteners, current leads, pipelines, storage tanks for cryogenic liquids, fuel, and de-icing systems, as well as in chemical reactors and ship structures.

## 2. The Physical Nature of the Production of Permanent Compounds of LMCM in the Solid Phase

Layered metal composite materials consist of two or more layers or plates of various metals connected in such a way that the properties of the resulting composition significantly exceed the properties of its constituent components. These materials can be pre-calculated and obtained with specified properties. Such properties include corrosion resistance, surface hardness, wear resistance, impact resistance, viscosity, strength, improved thermal and electrical conductivity, magnetic properties, controlled thermal expansion, elasticity, shape change, *etc*. The components of the composite material are selected in such a way that one (or more) of the above-listed required properties is achieved. For example, copper-clad corrosion-resistant steel is a good roofing material because each component improves the properties of the entire laminate. Copper provides appearance requirements and machinability, whereas steel increases strength and reduces the consumption of more expensive copper. In addition, the lower thermal conductivity of corrosion-resistant steel compared to copper improves the ability of the laminated material to solder. On the other hand, copper plating on corrosion-resistant steel improves heat transfer when used in cooling systems.

The mechanism of formation of an integral joint in the solid phase in Ref. [21] is divided into three stages: the formation of physical contact, activation of contact surfaces, and the development of interaction in the volume of contact zones. Several authors [22] have proposed several hypotheses and theories explaining the physical nature of the production of solid-phase compounds of metals and alloys in works related mainly to bimetallic materials since the 50s and 60s of the last century.

One of them is the crystallization hypothesis, according to which a durable compound is formed due to the formation of common recrystallization grains at the boundary of layers, where large deformations and local temperature increases are observed. However, according to the authors [23], this hypothesis does not explain the occurrence of the compound at very low temperatures, which excludes the possibility of recrystallization processes.

The diffusion hypothesis explains the connection of metals by diffusion processes in the contact zone, the intensification of which is facilitated by high pressure and the heat caused by it.

Dislocation theory relates the formation of a compound during the joint deformation of metals with their plastic flow in the contact zone caused by the deformation of microdimensions, the occurrence, and movement of dislocations leading to the formation of metal bonds.

The film theory is based on the assumption that for the formation of a compound, it is necessary to bring the pure (juvenile) surfaces of the joined metals closer to the interatomic interaction distance.

The energy hypothesis suggests that to form metal bonds, in addition to bringing the contact surfaces closer to a distance less than the interatomic one, the energy of the atoms must reach the so-called setting threshold, at which the electronic configurations of metal atoms are disrupted.

All existing hypotheses are scientifically substantiated and have an experimental evidence base. However, considering the new research results, a new interpretation of these theories and hypotheses is proposed about compounds obtained by explosion welding [23]. Thus, in Ref. [24], it was suggested that the formation of local melting zones and protrusions on the interface might serve as a mechanism for ensuring the adhesion of materials during explosion welding.

## 3. Methods of Obtaining of LMCM

The main methods for obtaining LMCM by combining the aggregate state at the boundary of the compound of the components are divided into solid-phase (pressure treatment), liquid–solid-phase (powder metallurgy), liquid-phase (methods of impregnation, extrusion in the liquid phase, layered casting and directional crystallization), gas-phase and electrochemical (deposition-spraying methods). In Refs. [25–32], the main methods of production of layered composites include foundry cladding, hot and cold plastic deformation (rolling, pressing, drawing, screw extrusion), explosion welding, electroslag surfacing, combined methods (casting + rolling, explosion welding + rolling, *etc*.), cumulative batch rolling with the connection of layers (ARB process) and equal channel angular extrusion (ECAE). The last two methods relate to the processes of intense plastic deformation (severe plastic deformation) or metaplastic deformation, which ensures the production of volumetric submicron- and nanocrystalline structures in metals and alloys.

When choosing materials for creating LMCM, it is necessary to proceed from their possible compatibility with each other. The work [33] provides a classification of materials by the nature of interaction with each other (metals with limited or complete insolubility with each other; metals with good solubility, and metals forming intermetallic compounds), based on which the optimal method for manufacturing layered metal-based composites is determined.

In the early 1970s, layered composites began to be manufactured by metal plating (cladding, *i.e.*, methods and technologies, which ensure the layered connection of metals and alloys to form a multilayer material). To obtain multilayer composites, such cladding technologies for metal, ceramic, and polymer materials as hot and cold rolling, pressing, double-layer casting, explosion cladding, cladding layer surfacing, *etc.* are used.

One of the planning methods is the joint hot rolling or drawing of the base and protective metals. Welding of two different metals and, thus, the formation of a layered composite was carried out due to their mutual thermal diffusion under the influence of the deformation of a pre-made billet.

Metals and alloys with good weldability are used for planning. These are carbon and acid-resistant steels, duralumin, and copper alloys. Aluminium, tantalum, molybdenum, titanium, nickel, and stainless steel are used as a protective coating. The cladding purpose is to create on the surface of the protected part a layer of material with higher performance properties, namely, high strength and corrosion resistance. The disadvantages of cladding are high cost and accelerated corrosion in the area of welded seams.

In the 1980s and 1990s, articles were published on the cladding of steels with various metals and alloys to enhance their mechanical properties. O.D. Sherby *et al.* [34] demonstrated the feasibility of solid-phase cladding at temperatures below the eutectoid transformation temperature of 727 °C, similar and other iron-containing alloys with a wide range of carbon concentrations, as well as the advantages of cladding at low temperatures.

Packages from a plate with a thickness of 2 to 4 mm in the number of 2 to 25 pieces were welded in two ways. The first is warm pressing at a pressure of 69 MPa at a temperature of 650 °C in air, in a vacuum or a protective atmosphere for 30 minutes to several hours. The composites were then subjected to either temperature forging or isothermal rolling with 5–10% compression per pass and annealing between passes. The second method is welding packages assembled from a large number of thin plates and pre-welded along the periphery with an electron beam in a vacuum, rolling at a temperature of 650 °C with compressions of about 3–10% per pass with annealing between passes. It was found that the setting of plates of various compositions is possible if one of the sets of iron-containing plates has increased plasticity.

In Ref. [35], a solid-phase diffusion setting of pure titanium with 304 stainless steel through epy 0.3 mm-thick copper layer was described, which was carried out in the temperature range of 850–950 °C for 1.5 hours under the action of a uniaxial load of 3 MPa in vacuum. The study aim was to the effect of welding temperature on the microstructure of the boundaries and deformation properties of the assembled packages. At temperatures of 850 °C and 900 °C, products of the triple Fe–Cu–Ti diagram were formed at both diffusion boundaries. When the welding temperature

increased to 950 °C, a weakening of the bond strength between titanium and steel was observed due to the formation of a brittle intermetallic phase Fe with Ti. The maximum bond strength of ≈318 MPa and deformation to fracture of ≈8.5% were obtained for a package welded at 900 °C. That was due to the better grip of titanium and steel on the touching surfaces. With an increase in the welding temperature to 950 °C, the bond strength between the components decreased due to the formation of brittle intermetallides at the interface.

The aim of the authors of the work [36] was to create thin composite foils from sheets of iron–aluminium alloy and sheets of chromium–molybdenum steel by cladding using their joint rolling at 873 or 1273 K. At the same time, the composition of the (Fe–Al) alloy (Fe–14 and 20 at.% Al) was controlled, and the deformation ability of the resulting composite was evaluated. The ability of the composite to deform was evaluated by three-point bending tests at room temperature. Regardless of the composition of the (Fe–Al) alloy, composite plates welded by rolling at 1273 K had a higher deformability than the same composite plates obtained at 873 K. Then the plates were rolled into a thin tape at room temperature to a thickness of 0.12 mm and a length of up to 670 mm, which corresponded to a deformation of 99.8%. The texture of the rolled clad composites became more acute with an increase in the degree of deformation and a decrease in the aluminium content in the Fe–Al alloy.

In Ref. [37], a package assembled from aluminium and steel strip elements was rolled to obtain a multilayer composite with improved properties, also the temperature and time effect of subsequent annealing on the layered structure and mechanical properties of this composite were investigated. Local thickness decreases, and ruptures of steel layers occurred already on the 2$^{nd}$ cycle of batch rolling due to the difference in the ability of aluminium and steel layers to deform. The microhardness values of both layers increased sharply at the initial stages of joint rolling, but then the microhardness remained constant for steel, and for aluminium, it slowly increased. Heat treatment at 500 °C led to the formation of intermetallic phases at the boundaries of the steel and Al layers, which, as expected, caused a decrease in tensile strength and yield strength. As the annealing time increased, the thickness of the intermetallic phase increased, and, as a result, the elongation decreased.

Authors of Ref. [38] describe a multilayer NbTi/Nb/Cu composite based on a superconducting Nb–50 wt.% Ti alloy in the form of a 1 mm-thick multilayer bus and inside hollow multilayer cables. The tyres were produced by successive hot and cold rolling of flat multilayer packages. Cables were obtained by deep drawing and drawing of specially assembled tubular cylindrical blanks.

In Ref. [39], explosion welding is described as a high-intensity short-term effect accompanied by the phenomena of wave formation, cumula-

tion, and setting of bodies and is comparable in its effect to the processes of severe plastic deformation (SPD), realized in a narrow contact area and leading to fragmentation of the structure. The physical foundations of the formation of a strong joint by high-speed collision are also described in detail, *e.g.*, in Refs. [40–43].

Explosion welding, according to the authors [39] and others, refers to the most effective method of creating high-quality composite materials of various types and purposes. Due to its transience, the explosion welding process prevents the development of active diffusion processes in the joint zone and allows you to obtain equally durable compositions from almost any dissimilar metals. It is noted in Ref. [44] that explosion welding is indispensable for obtaining high-strength composites from dissimilar materials such as aluminium–steel, aluminium–copper, aluminium–titanium, titanium–steel, zirconium–steel, and others, which tend to form brittle intermetallics, sharply reducing the strength of the joint. According to the data of works [45–47] devoted to the study of LMCM obtained by explosion welding with micro- and nanoscale layers, the number of layers in a package for one explosive loading can reach 50. The advantages of explosion welding, as a technology for producing LMCM, include the possibility of preserving the original structure of the layers of the composite components. During the manufacture of LMCM using explosion-welding technology, in addition to creating a durable connection of the layers, the hardening of the composite layers caused by the propagation of shock waves in the metal volume is achieved as a side effect. The achieved hardening is reflected in an increase in microhardness in the near-seam zone, followed by a gradual decrease as it moves away from the seam boundary. At the same time, it is also possible to soften the metal caused by its heating due to an increase in the thermal component of the shock wave at high pressure.

Diffusion welding by pressing in the production of LMCM is carried out at a temperature below the melting point of the metals to be welded with the application of pressure necessary for plastic deformation of the contact layers and the formation of chemical bonds due to mutual diffusion between the atoms of the surfaces to be joined. The pressing of LMCM by diffusion welding involves the preparation of the surfaces to be joined, heating, implementation of compressive loads, isothermal exposure, and cooling. To create a durable one-piece joint in LMCM, diffusion welding is recommended to be carried out in vacuum or protective and reducing atmospheres [48].

The basics of obtaining LMCM by the high-tech method of hot and warm batch rolling are described in detail in Ref. [9]. This method is focused on multi-scale production, and its use makes it possible to achieve high deformation compressions. Despite several advantages, batch rolling also has some disadvantages, which are mentioned in Refs. [18, 22]. These include the complexity of preparing the package before compression, in-

stability of the joint quality, heterogeneous deformation of dissimilar materials, and their oxidation during rolling.

Deformation of LMCM based on low-carbon steels by rolling with high degrees of deformation can lead to embrittlement of the material, sharp exhaustion of the plasticity resource of the material, and, accordingly, delamination of the material under the influence of significant residual stresses both along the interface of the layers and along the central part of the most durable layer [49].

The results of the research show that attempts to obtain a multilayer structure by hot rolling based only on iron layers lead to the formation of a monologging without visible signs of a multilayer laminar structure. To gain an LMCM with high strength and without violating its layered architecture, the following points must be considered. As shown [50–55], the preservation of the layered structure in the workpiece is possible if steels with different crystallographic structures (b.c.c. and f.c.c. lattices) participated in the initial composition. Long-term exposure of the package and high hot rolling temperatures above 1050 °C, as shown by the example of layered composites based on 40X13 and 08X18H10 steels, as a result of active diffusion processes during hot deformation, leads to a violation of the laminar structure of the interlayer boundaries and the concept of a layered material loses its physical meaning.

In Refs. [56, 57], attention is paid to the fact that when rolling reaches a certain degree of deformation of the LMCM, local thinning of more plastic layers is possible, and further deformation can lead to fragmentation of the layers and, consequently, a violation of the laminarity of the structure and the transition of the composite from the layered type to the matrix type. Batch rolling can be used as one of the stages of a combined technology for producing LMCM (diffusion welding + batch rolling; explosion welding + batch rolling).

The SPD method, which consists of deformation with large degrees of deformation at relatively low temperatures ($0.3–0.4T_{melt}$) under high-applied pressures, provides the production of bulk non-porous nano- and sub microcrystalline metals and alloys. Among the main SPD methods used to obtain LMCM in a solid-phase state, equal-channel angular pressing and accumulative roll bonding (ARB) processing can be distinguished. The ARB process is a type of batch rolling proposed by the authors [58] and is a multi-pass rolling process, in each cycle of which the sheet blank is compressed by 50% and then cut and assembled into a package for subsequent passage.

The ARB process related to SPD methods is carried out at a temperature below the recrystallization temperature, which makes it possible to create a submicron- and nanocrystalline structure in metals and alloys, as well as to ensure a high level of strength properties [59].

In Ref. [60], the ARB process at room temperature is used to produce a sheet aluminium-matrix composite reinforced with $Al_2O_3$ and $B_4C$ nano-

particles. A variation of the ARB process is the CRARB process (cross-roll accumulative roll-bonding process), the feature of which is to change the orientation of the sheets by 90° relative to each other between successive rolling cycles (Fig. 1). Using this method, LMCM was obtained from the initial rolled aluminium sheets and powder materials SiC, $B_4C$ [61, 62]. This technology provides a higher range of mechanical properties of composites compared to the ARB process; however, the thickness of the resulting sheet-layered composites does not exceed 1 mm.

LMCM is made with a basis of monolithic sheet and composite materials belonging to fibre metal laminates (FML) for structural and functional purposes [18] and represents a 'composite within a composite' where metal matrix interlayers with alternating sequence together with monolithic materials organize the structure of a layered composite. Advanced casting and powder metallurgy methods are mainly used to obtain functional metal matrix composites. To gain a monolithic nanostructured or aluminium composite, R. Vintila *et al.* [63] used a complex technology of cryogenic grinding of powders and their subsequent plasma sintering. The physical foundations, methods, and features of powder rolling are presented in detail in [18].

According to the results of the study [64], to obtain high-quality nonporous layers during rolling, powders must be in a liquid-solid state. At the same time, the proportion of the liquid phase in powder particles, according to various estimates, should be 35-60%. For the first time, the authors of attempted to obtain a layered hybrid composite (borate) based on external aluminium layers and a central powder layer consisting of a mixture of aluminium powders and boron carbide. Another deformation method for producing or aluminium composite involves the utilization of a closed steel shell when rolling a package. In this case, steel acts as a formative protective frame, which is removed at the end of deformation. It should be noted that according to the data available in the available literature, high-performance batch rolling methods for producing layered boroaluminium neutron-protective composites have not been still used in many developing countries.

It is particularly possible to highlight the works devoted to the preparation of layered composites using accumulative roll-bonding (ARB). In such works, it is customary to investigate changes in the microstructure and control the physicomechanical parameters of composites depending on the number of cycles, which can be up to 10 pieces. ARB is successfully used for the manufacture of layered composites, the components of which are well-deformable metals or alloys. These include nanocomposites Cu/Nb [65, 66], Cu/Ag [23], Cu/Zn [67].

Layered Cu/Nb composites studied in Ref. [65] had, perhaps, the widest range of variation in the thickness of copper and niobium layers, $h$, from 0.7 μm to 7 nm. As $h$ decreased, the hardness of the composites increased from 1.8 (at $h$ = 0.7 μm) to 4.5 GPa (at $h$ = 7 nm).

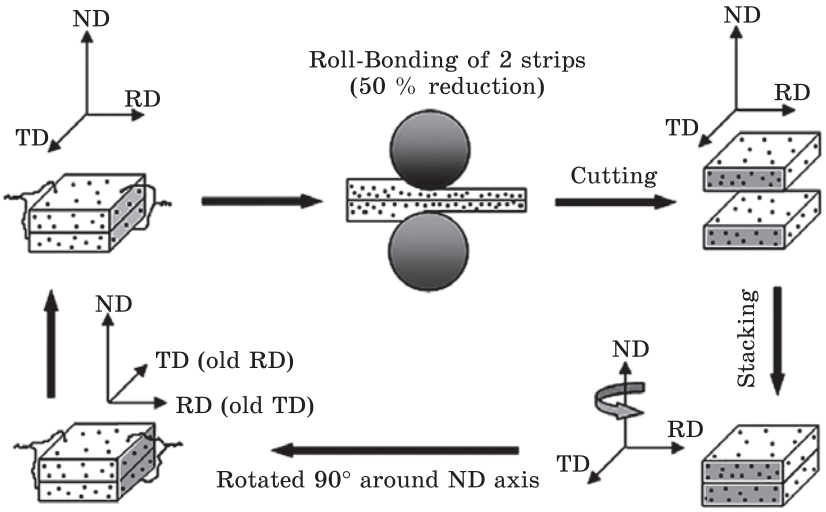


*Fig. 1.* Cross-roll accumulative roll bonding process [62]

The hardness of the composites increased from 1.8 to 4.5 GPa as the layer thickness decreased from 700 to 7 nm. The tensile strength of a layered nanocomposite with a thickness of 58 nm layers was 1 GPa and increased to 1.78 GPa at $h$ = 18 nm.

The results obtained in Ref. [66] are of interest. Cu/Nb nanolaminates with 18 nm thick layers after ARB were subjected to large deformations by torsion under high pressure at room temperature. Microstructural studies have shown that the layered morphology of the composite resisted torsion up to a relative deformation of ε equal to ≈11. As the torsion continued to deform, the 3-dimensional microstructure characteristic of torsion replaced the original layered structure of the composite. The average grain size of copper and niobium decreased to 5 nm at ε = 286. It has been shown that in the border regions, Nb is dissolved in Cu (up to 1.5 at.%) and dissolution of Cu in Nb (up to 10 at.%), but the formation of new phases, including amorphous ones, was not observed in the composite.

Nanocomposite 'multilayers' of Cu/Ag [68] were studied to assess the possibility of their use in special electrical devices, where it was required to provide a conductor with high strength and at the same time maintain high electrical conductivity comparable to that for individual conductors made of copper and silver. Ultrathin grain structures were observed in Cu/Ag composites after the 5$^{th}$ cycle of ARB.

Composed of individually fragile sections of copper and silver tapes with a thickness of 200 and 100 μm, respectively, Cu/Ag composites after the 9$^{th}$ cycle of ARB had a tensile strength of 660 and 640 MPa if the thickness of the 'multilayer' was 0.2 and 0.1 mm, respectively. That was several times higher than the tensile strength of individual bands of cop-

per or silver. The layer's integrity was maintained due to the high deformation capacity of each component. That provided the composite with electrical conductivity no worse than in massive conductors made of copper and silver.

However, a slight increase in electrical resistance in samples with an initial thickness of silver layers equal to 100 μm, compared with a composite of Ag foils with a thickness of 200 μm, nevertheless took place. The decrease in electrical conductivity was explained by the scattering of conduction electrons on the interface surfaces between the layers, the density of which reached a specific critical value.

In Ref. [67], the microstructure of multilayer Cu/Zn micro composites obtained over 8 ARB cycles is studied, and the results of measurements of the microhardness *HV* of individual Cu and Zn layers and tensile strength tests after each ARB cycle are presented. The package for the 1$^{st}$ cycle was made up of Cu and Zn strips measuring 50–150 mm$^2$ annealed at 500 °C for 1 hour for copper and at 150 °C for 30 minutes for zinc. The annealed strips were washed with acetone and cleaned with wire brushes to roughen their surface. The package was assembled by alternating two Cu and one Zn strips with a thickness of 1 mm. Initially, it was rolled at room temperature with 57% compression in one pass. Then it was cut into 2 parts, cleaned again, folded, and fixed at the edges with copper wire. The setting of such a two-layer assembly was carried out by rolling at room temperature with 50% compression. This was repeated 8 times in a row. The contact surface between the layers remained straight for 3 cycles. After the 4$^{th}$ cycle, local thinning of the layers appeared, and the interface surfaces acquired a wavy character. After the 5$^{th}$ cycle, the copper layers thinned even more, creating lens-like fragments in the microstructure. In addition, the formation of $CuZn_5$ intermetallic compound, microcracks at the interface, and Kirkendall's pores in the zinc layer were observed in the composite structure during the ARB. Depending on the cycle number, the tensile strength first increased to a maximum value of 280 MPa and then fell, and the hardness of both layers increased. In the early stages of ARB, defects of a 'dimpled' nature could be observed in both layers.

Metallic layered composites with nanometer-scale structural components attract the attention of researchers with their unique properties inherent in the nanoscale structure and the prospect of their practical application. Traditionally, such multilayer composites were made using one of the 'layer-on-layer' deposition methods. The repetitive pressing and rolling operations method makes it possible to produce multilayer structures from solid metal powders and sheets. Here, the pressing operation is understood as the effect of pressure on the package located between two punches. That is diffusion welding under pressure.

Nanoscale metal 'layers' of Fe/Ag [69], known for high magnetoresistance, were obtained in 3 cycles, each of which consisted of pressing at

573 K in vacuum and rolling in air with intermediate 1-hour annealing at 873 K. The magnetic resistance of the resulting composite was measured at 5 K when an electric current $I$ was passed perpendicular ($\perp$) and parallel ($\parallel$) to the plane of the layers ($ab$). In a composite with an Ag layer thickness of ≈10 nm, a gigantic magnetoresistance equal to 13% was observed at $I \perp (ab)$. At $I \parallel (ab)$, it was 4%. There was a clear relationship between the thickness of the Ag layer and the ratio of magnetoresistance. The critical thickness of the layer demonstrating such magnetoresistance was 100 nm. Fe/Ag and Fe/Cu nanolaminates with layer thicknesses of 20 nm were obtained using multiple cycles of diffusion welding-vacuum pressing and rolling in Refs. [70, 71] to study their magnetoresistance. A magnetoresistive effect similar to that found on the same nanolaminate manufactured by CVD (chemical vapour deposition) was obtained on Fe–Cu samples. This result indicates the prospects of purely metallurgical techniques for obtaining massive magnetoresistive nanolaminates. Their performance significantly exceeds the capabilities of the CVD method.

In Ref. [70], high-strength layered Fe/Cu nanocomposites were obtained from foils of iron and copper, metals that do not differ in high strength. We used three cycles. The cycle consisted of pressing at 673 K in a vacuum and rolling at room temperature with intermediate annealing at 873 K for 1 hour, also in a vacuum. As the thickness of the layers decreased, the strength measured at room temperature increased to a maximum value of 1.57 GPa with a relative elongation of ≈0.75%.

Using the same method, Cu/Nb composites with bulk niobium contents of 15.6%, 25%, and 36.3% and Ti/Al [71] were also obtained from metals that were well deformed at room temperature. The nanoscale thickness range of Cu and Nb layers occurred after relative deformations of 99.98%. At the same time, a sharp rise in strength values was observed, comparable to the strength of stainless steel. The relative elongation of the test samples increased with an increase in the number of 'pressing + rolling' cycles and with a decrease in the volume fraction of niobium. If the latter can be explained by the faster hardening of niobium compared to copper as the degree of deformation increases, then the former turned out to be an unexpected and, therefore, non-trivial result.

Layered Ti/Al composites [71] with volumetric aluminium contents in the range from 10 to 67% showed a good combination of strength, density, and especially plasticity. The elongation for all composites was high and amounted to 30–40%.

## 4. Features of the Formation of the LMCM Structure

The patterns of structure formation at the interface of layers and in the near-seam zone of explosion-welded permanent joints of dissimilar and opposite metals and alloys were primarily revealed using the example of bi-

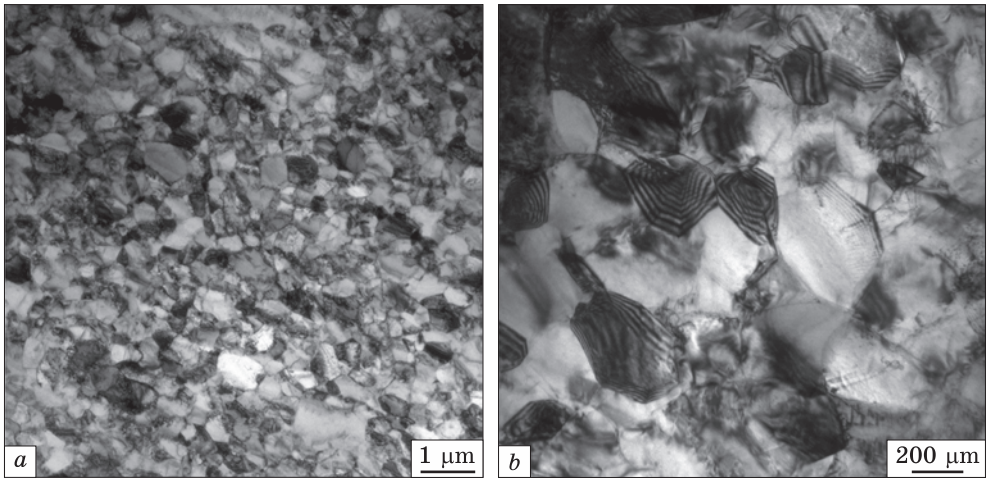


*Fig. 2.* Ferrite grains (at different magnifications) formed during explosion welding process [79]

metallic materials. However, these patterns can be significantly extended to multilayer composites. During explosive loading, such complex processes as wave formation, strong plastic flow, formation of vortices, reflow zones with a cast or UFG structure [72–76], as well as zones with relatively homogeneous recrystallized and strongly deformed grains occur at the junction boundary and in the near-seam zone, which is established in the works [24]. The boundary of welded joints obtained by explosion welding is most often characterized by a wave-like structure, but there are also straight welds. It was found in [77] that the length and amplitude of the waves depend on the technological parameters of explosion welding (angle and velocity of impact, the distance between the plates being thrown, *etc.*), the geometry of the plates being connected, and according to work [28] also largely on the crystallographic orientation of the grains involved in their construction. The structural features of vortex zones and near-arc zones formed during explosion welding of heterogeneous materials were studied in Ref. [78], where micro-volumes characterized by an amorphous structure are formed in the mixing zones of steel and titanium. B.A. Greenberg *et al.* [24], for the first time, discovered, using the example of compounds of dissimilar materials obtained by explosion welding, and described in detail the fragmentation process of the crushing type, which is the separation or closure of component particles at the junction boundary under the action of an explosive wave.

The details of the fine structure of vortices and the near-seam zone of the welded joint of steel multilayer materials were studied in Ref. [79] (Fig. 2). At the same time, the issues of structure formation in the part of the layers removed from the boundary of the welded joint of layered com-

posites have not been sufficiently studied. The exception is the work [78], in which, using the example of layered welded composites based on steels 20, 08kp, 45KHNM, 12X18H10T, 5KHV2S and H18K9M5T, several zones with different types of fine structure were identified as they moved away from the boundary of the welded joint (70–150 μm), and the formation of bands of localized plastic deformations. In the central part of the 08kp layers, the main feature of deformation hardening of steel layers is twins of deformation origin.

Shear deformations during batch rolling lead to the appearance of an elongated grain structure in LMCM. The completeness of the DR flow, which consists of the formation of the new grain, is largely determined by the temperature and degree of deformation of the LMCM layers. In the works devoted to ARB-rolling of plastic materials after 6–8 cycles, the formation of a UFG structure is noted in a multilayer billet [80, 81]. In Refs. [80, 81], the category of UFG structures includes a structure in which the average grain size is less than 1 μm in at least one direction, while the length of the grain in the other direction may exceed this value. A common feature of such structures when observing multilayer materials in the longitudinal direction concerning the rolling direction (RD) is the formation of grains with a diameter of less than 1 μm with clean but sinuous boundaries. In the transverse rolling direction (TD), all materials are characterized by an elongated grain morphology, which is conventionally called 'pancake UFG', if the grain is moderately elongated, and 'lamellar boundary structure', if the grain is strongly elongated.

If, in the case of cold and warm rolling of LMCM, the formation of the final structure in the layers occurs as a result of successive deformation, heating, and cooling operations, then, in the process of hot rolling of LMCM, these are the cooling conditions, which will be an essential factor. The course of collective recrystallization at the end of rolling eliminates all the beneficial effects achieved by plastic deformation. However, to date, the issues of the evolution of the grain structure of metal under the influence of various schemes of plastic deformation, temperature, and conditions of limited metal flow, including as part of a multilayer package, have not been systematically studied.

Essential characteristics of the microstructure of powder materials are the presence of pores, grain size, and the degree of uniformity of the grain structure. These characteristics can be controlled by external influences (pressure, temperature, medium, heating rate, and exposure), knowing the physicochemical nature of the components of the powder mixture. The hot rolling technology can be used as an effective method of creating a monolithic, practically non-porous material, including simultaneously the stages of compaction and sintering of powder particles. The processes of structure formation in powder bodies during rolling are complex and are described in detail in Ref. [81]. It should be noted that most micro-

structural studies of metal matrix composites are limited to studying the distribution pattern in the boron carbide matrix, porosity assessment, and morphology of the initial powder particles by scanning electron microscopy. Structural studies of metal matrix composites using back-reflected electron diffraction and transmission electron microscopy (TEM) methods are presented in several papers [82–84]. The authors [85] used the TEM method to study in detail the fine structure of an aluminium matrix composite with additives of boron carbide particles and found that samples with 10% $B_4C$ recrystallize at a temperature of 350 °C, while samples with 25% $B_4C$ retain the nanostructure and do not recrystallize up to annealing temperatures of 550 °C.

In Ref. [82], using the example of an $Al/Al_2O_3/B_4C$ composite obtained by the ARB process, based on structural studies by the TEM method, it was shown that the presence of nanoparticles of 1.3 wt.% $Al_2O3$ and $B_4C$ in the aluminium matrix leads to grinding of the matrix grain and an increase in dislocation density in it. It is important to note that the use of thin powder layers of $B_4C$ in the composition of layered composites obtained by cumulative batch rolling leads to the introduction of powder particles into monolithic aluminium sheets without the formation of separate powder layers [62, 85]. At the same time, the results of structural studies [84] of hot-rolled aluminium matrix composites with reinforcing $B_4C$ particles are not presented in the available literature.

## 5. Physical, Mechanical, and Functional Properties of LMCM

It is known [86, 87] that due to the combination of heterogeneous and non-durable materials in the package structure, the presence of a layered composite architecture, as well as the use of hardening methods of deformation and heat treatment in LMCM, a unique complex of physical and mechanical properties can be obtained.

The strength of layered composite materials is more closely related to the properties of hardeners in a massive cross-section than to the properties of small-volume (one-dimensional) hardeners such as whiskers (filamentous crystals) or fibres. Since the reinforcing plates have two sizes that are comparable in size to the dimensions of structural parts, defects in the reinforcing component can be the nuclei of cracks with a length comparable to the length of cracks in the part. This effect of defects in a lamellar composite material is the opposite of the effect that defects have on the formation of cracks in fibrous composite materials. In fibres under tensile axial load, the crack propagates in the transverse direction since the cross-sectional area of the fibre is small compared to the surface of the entire sample [88–91].

The crucial reinforcing materials are inherently brittle, and their strength is related to the statistical distribution of defect density and in-

tensity. Such reinforcing phases obey the classical destruction mechanism established by Griffiths, and their strength is inversely proportional to their size. The strength of layered structural composite materials is limited to some extent by the lower strength of the reinforcing layers (foils) compared to fibres. In addition, the low amount of deformation during the destruction of the brittle reinforcing phase limits the elongation and plasticity of the composite material in all directions and the reinforcement plane. However, the strength and modulus of elasticity of the reinforcing phase are realized in all directions of the plane, which gives significant advantages compared to unidirectional fibre reinforcement.

Compared with the initial components, LMCM of various compositions in a wide temperature range have an increased level of mechanical properties during uniaxial tensile tests. The actual strength of these materials, in some cases, may exceed its theoretical values calculated according to the rule of mixtures (rule of additivity). For example, the fixed strength level of composites obtained by explosion welding technology exceeds the values of the tensile strength and yield strength calculated according to the rule of mixtures by 1.26 times and 2.32 times, respectively. However, the rule of mixtures may be violated when a fragile component appears in the system. A significant influence on the strength properties of layered composites is exerted by the quality of the connection of the layers, which is ensured by the presence of interatomic bonds between the atoms of the connected surfaces in a state of physical contact. The adhesion strength of the layers should not be lower than the strength of the metals, which make up the composites, and is evaluated according to the results of shear tests by state standard 10885-85 or separation. The reason for the insufficient strength of the joint in the LMCM obtained by batch rolling may be an undesirable embrittlement phase that occurs at the boundary of the connected components at the manufacturing stage of some layered composites, the presence of iron oxide, pores, and irregularities, which is almost completely excluded in the case of explosion welding technology. However, as found in Ref. [78], during explosion welding of titanium alloy BT23 and steel 08kp, small crystallites of intermetallics form in local areas of the welded joint. The effective use of intermediate layers protecting the boundaries of welded joints from the formation of the brittle intermetallic is shown in [47] in the example of a layered Ti/Ta/Cu/Ni composite obtained by explosion welding. During explosion welding, microhardness increases in the near-seam zone with its subsequent decrease as it moves away from the seam boundary. At the same time, it is also possible to soften the metal due to its heating due to an increase in the thermal component of the shock wave at high pressure.

Giving LMCM an increased level of mechanical properties is possible due to the use of SPD methods during the direct manufacture of the composite [92]. However, deformation methods for obtaining LMCM do not

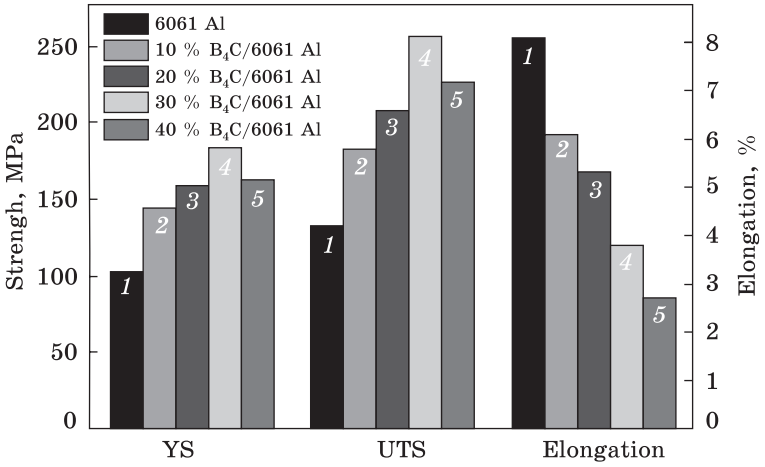


*Fig. 3.* Tensile strength of aluminium alloy 6061 depending on the content of $B_4C$ particles [83], where YS and UTS denote yield strength and ultimate tensile strength, respectively

always lead to an increase in strength indicators. The opposite dependence can also take place, when, as deformation accumulates in LMCM with each new rolling cycle, a decrease in yield strength associated with the processes of dynamic return and recrystallization can be observed.

Among the main factors that form the mechanical properties of tensile steel–aluminium and steel-layered composites with the same technology for their production, it is possible to distinguish the mechanical characteristics of the composite components, taking into account their changes during deformation and heat treatment, as well as their volume fraction. The use of interlayers of high-strength martensitic-aging steels X15N5 and H18K8M5T in three-layer compositions in combination with the ACMg alloy with a volume fraction of steel components of 54–77% made it possible to increase the values of temporary tear resistance to the level of 1230 and 940 MPa, respectively [27]. A higher level of strength ($\sigma_B$ = 1510–1810 MPa) was achieved in 2- and 13-layer welded composites based on martensitic-ageing steel H18K9M5T, austenitic steel 12X18H10T and steel 20 after additional exposure at a temperature of 490 °C for 3 hours. According to, in a multilayer composite (up to 2000 layers) based on 08X18H10 and 08X18 sheets of steel with an average thickness of about 1 μm, temporary tear resistance $\sigma_B$ = 800 MPa is achieved, which is 1.6–1.7 times higher than the strength of the initial components of the composite.

The data on the mechanical properties of metal-matrix Al/$B_4C$ composites [62, 83, 93] have a wide range of values ($\sigma_B$ = 69–470 MPa), primarily related to the different content of the volume fraction of boron carbide, the grade of aluminium alloy and the technological features of producing composites. According to the results of mechanical tests of the Al/$B_4C$ composite based on the aluminium alloy Al6061, the authors [83] showed that an increase in the content of boron carbide particles over 30% leads to a decrease in the strength characteristics of the material (Fig. 3).

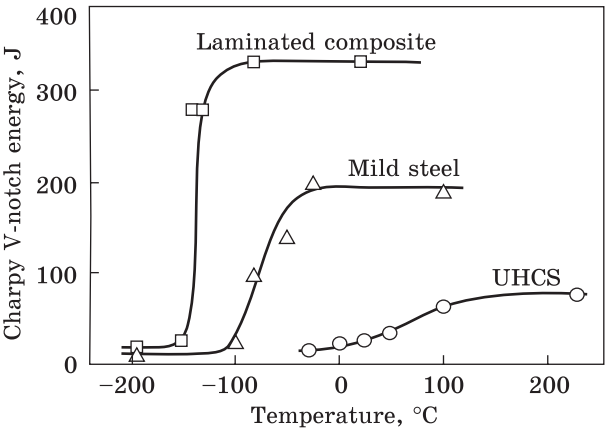


*Fig. 4.* Temperature dependence of the fracture work of high-, medium-carbon steels and LMCM based on them during impact tests from –200 °C to +200 °C [97]

Conducting modern instrumented impact bending tests allows us to obtain detailed information about the mechanism and energy intensity of the process of destruction of monolithic, as well as composite materials. The fracture resistance of LMCM during toughness tests significantly depends on the orientation of the incision line relative to the plane of separation of the layers. In Ref. [94], three main types of the arrangement of the joint surfaces in LMCM are analysed, ensuring the separation of the crack-divider, its crack-arrester, and the passage of a through crack along one of the interlayer boundaries. The maximum resistance to impact fracture of a layered material is achieved if the load is perpendicular to the plane of the interface of the plates, *i.e.*, in the case of a crack-inhibiting arrangement of layers, as shown by the authors of works [93].

An increase in the bond strength between the layers, *i.e.*, an increase in the 'degree of solidity' of the layered material, leads to a decrease in the impact strength of the composite in the case of a crack orientation according to the braking type. Conversely, the presence of weakened interface surfaces in a composite layered material, as in [95], increases the resistance to impact destruction of the material.

The behaviour of high- and medium-carbon steels and a 12-layer composite based on them with an incision orientation according to the braking type under shock loading at temperatures from –200 to +200 °C is clearly shown on the temperature dependence of the fracture work of impact samples of these materials (Fig. 4) [96, 97].

The layered composite demonstrates high resistance to influence fracture in the temperature range from –150 °C to +20 °C, which is associated with the formation of stratifications along the boundary of the layers on both sides of the main crack. An increase in the impact strength and a shift in the temperature of the ductile–brittle transition to the region of lower temperatures in layered composites can be also observed. It should be noted that a comparative assessment of the impact strength characteristics at room and low climatic temperatures of LMCM of the same composition and design, but obtained using various technologies, has not previ-

ously been carried out. The impact strength of $Al/B_4C$ composites with a powder content of $B_4C$ of 5, 10, 15, and 20 wt.% obtained by pressing under pressure at various temperatures was observed as well. At the same time, there is a tendency to decrease the density and toughness of the material with an increase in the boron carbide content and an increase in the pressing temperature. At the same time, the results of instrumented impact tests, which allow us to judge the stages of the process of dynamic destruction of hybrid $Al/B_4C$ composites, are not given in the scientific and technical literature.

According to the results of Refs. [86, 87], the multilayer structure, the optimal combination of components and methods of shaping and additional deformation and heat treatment, in addition to an increased complex of mechanical properties and resistance to brittle fracture, gives the composite specific magnetic, thermophysical and various functional properties.

In Ref. [96], the possibility of using the maximum value of differential permeability as a parameter in the diagnosis of the formation of a magnetically ordered phase in austenitic steels, as one of the components of the layered material 'austenitic steel–ferritic (ferrite–pearlite) steel' in the process of elastoplastic deformation was revealed. Magnetic characteristics have been established that can be used to assess the stress–strain state of both the entire composite as a whole and its layers during elastoplastic deformation. It should be noted that the obtained results of determining the magnetic properties relate, as a rule, to bimetals or layered materials with no more than 3 layers. As known, in the case of layered materials, the metallic (semi-conductor) properties of each layer can be changed into semi-conductor (metallic) ones through applied strain (as well as in monolayer materials) [98–112].

Such a crucial property of LMCM as thermal conductivity is determined by their structural and mechanical heterogeneity and is usually an order of magnitude lower than the thermal conductivity of the initial components. The main factors influencing the thermal conductivity of LMCM include hardening zones formed during the manufacturing process near the junction boundary and in the volume of the layers, the presence of individual inclusions, pores, discontinuities, and diffusion interlayers at the interlayer boundaries that occur during heating and pressure treatment. It is noted that the decrease in the thermal and electrical conductivity of LMCM based on titanium and aluminium obtained by explosion welding technology with subsequent rolling is associated with the appearance and growth of diffusive intermetallic interlayers, which have lower thermophysical properties than the initial components of LMCM.

For layered hybrid materials with the function of radiation protection according to, the crucial thermophysical characteristics are the coefficient of linear expansion, thermal and thermal conductivity, heat capacity and

neutron transfer index (neutron flux attenuation coefficient), the values of which largely depend on the chemical composition of the materials used, the dispersion of powder mixtures, as well as the technology for producing composites. Data on the thermophysical properties of neutron-protective boroaluminium composites are presented in fragments in the available literature. The results of the study of powder mixtures of radiation-protective aluminium composites $AMg_6$/BN/W, B95/BN/W, $AMg_6$/$B_4C$/W, and B95/$B_4C$/W obtained by hot extrusion revealed high wear resistance and thermal conductivity of these materials with a neutron-radiation attenuation coefficient of 2.2–3.0.

As indicated in the literature, the thermal conductivity level of neutron-protective boroaluminium composites $\lambda$ to ensure heat dissipation during the natural cooling of fuel assemblies should be at least 1.2 W/(m×K). Aluminium matrix composites reinforced with nanoscale particles of $Al_2O_3$, SiC, TiC, $TiO_2$, $B_4C$, $TiB_2$, and WC have high tribological properties. The efficient possibility of using layered metal matrix materials to provide ballistic protection of products and structural elements is noted by the authors of Ref. [113].

Crucial properties of corrosion-resistant bimetals also include thermal conductivity and manufacturability, *i.e.*, the ability of the resulting bimetal to undergo further processing (stamping, bending, drawing, welding, *etc*.). The thermal conductivity of a bimetal with a cladding layer of corrosion-resistant steel is slightly lower than the thermal conductivity of the steel of the main layer and 2–3 times higher than the thermal conductivity of corrosion-resistant steel, which is very significant when manufacturing heat exchange equipment, including for the service sector.

The ability of bimetal, especially its cladding layer, to resist corrosion in a particular environment determines the areas of its possible application.

Bimetals for the deep drawing must combine high strength and sufficient ductility as well as good thermal conductivity and corrosion resistance. Such requirements are met, in particular, by bimetals such as steel + + copper and steel + nickel alloys, which make it possible to obtain products by deep drawing with the required physicochemical, mechanical, technological, and operational properties. These bimetals are well subjected to subsequent technological operations: stamping, bending, drawing, welding, and heat treatment, which have led to their widespread use in various components and mechanisms of a diversity of machines, apparatuses, and structures.

The purpose of the base layer in these bimetals is to provide the required ductility during extraction, strength, resistance to shock loads, *etc*. The principal role of the cladding layer is to guarantee high corrosion resistance and sufficient ductility during deep drawing operations. In addition, the cladding layer of copper and its alloys serves as a lubricant during sheet stamping operations. Based on these requirements, low-car-

bon steels with carbon content of 0.05–0.20% and with a small amount of impurities are recommended as the main layer of bimetals: 0.25–0.50% Mn, <0.10% Si, <0.04% S, <0.035% P, <0.15% Cr, <0.20% Cu, <0.30% Ni. These requirements are met by boiling steel (11kp, 18kp) and aluminium-deoxidized ageless steel (11UA, 18UA). Of the materials used as a cladding layer, copper and single-phase brass, as well as nickel and its alloys, are most often used. The most common materials for the production by the deep drawing method are three-layer tapes of brass + steel + brass and nickel + steel + nickel produced by cold roll cladding.

## 6. Summary

With the development of technology and production, composite materials have become a priority in comparison with traditional ones. Metal-based composite materials have a unique set of operational properties and are successfully used in such industries as aircraft engineering (for cladding, spars, panels, *etc.*), mechanical engineering (engines, compressor blades, and turbines, *etc.*), space technology for components of power structures of devices subjected to heating, mining (drilling tools, details of combines, *etc.*), construction (bridge spans, elements of prefabricated structures of high-rise structures), *etc*. Today, composite utilization makes it possible to reduce the weight of aircraft, cars, and ships, increase the power of engines, power, and transport installations, create new structures with high performance, and meet safety requirements. In addition, their use allows not only to increase the reliability and durability of parts and equipment, but also to reduce the consumption of high-alloy steels and scarce and expensive non-ferrous metals (Ni, Cu, Cr, Mo, *etc*.), thereby, reducing the cost of installations made from them. At the same time, with the use of composites, it is possible to reduce the cost of maintenance and repair of equipment.

REFERENCES

1. A. Denissova, Y. Kuatbay, and Y. Liseitsev, *Case Studies in Construction Materials*, **19**: e02346 (2023); https://doi.org/10.1016/j.cscm.2023.e02346
2. A. Volokitin and D. Kuis, *Journal of Chemical Technology and Metallurgy*, **56**: 643 (2021).
3. I.E. Volokitina, A.V. Volokitin, M.A. Latypova, V.V. Chigirinsky, and A.S. Kolesnikov, *Progress in Physics of Metals*, **24**, No. 1: 132–156 (2023); https://doi.org/10.15407/ufm.24.01.132
4. A. Naizabekov and E. Panin, *Journal of Materials Engineering and Performance*, **28**, No. 3: 1762 (2019); https://doi.org/10.1007/s11665-019-3880-6
5. I.E. Volokitina, A.V. Volokitin, and E.A. Panin, *Progress in Physics of Metals*, **23**, No. 4: 684–728 (2022); https://doi.org/10.15407/ufm.23.04.684

6. A. Bychkov and A. Kolesnikov, *Metallography, Microstructure, and Analysis*, **12**, No. 3: 564–566 (2023); https://doi.org/10.1007/s13632-023-00966-y
7. N. Zhangabay, I. Baidilla, A. Tagybayev, Y. Anarbayev, and P. Kozlov, *Case Studies in Construction Materials*, **18**: e02161 (2023); https://doi.org/10.1016/j.cscm.2023.e02161
8. I.E. Volokitina, *Metal Science and Heat Treatment*, **63**, Nos. 3–4: 163 (2021).
9. A. Volokitin, I. Volokitina, and E. Panin, *Metallography, Microstructure, and Analysis*, **11**, No. 4: 673 (2022).
10. I.E. Volokitina, *Progress in Physics of Metals*, **24**: No. 3: 593–622 (2023). https://doi.org/10.15407/ufm.24.03.593
11. V. Bilous, V. Borysenko, V. Voyevodin, S. Didenko, M. Ilchenko, O. Rybka, O. Kuznetsov, and Y. Plisak, *Journal of Materials Science and Chemical Engineering*, **2**: 6–11 (2014); https://doi.org/10.4236/msce.2014.28002
12. S.V. Gladkovskya, I.S. Kamantsev, S.V. Kuteneva, D.A. Dvoynikov, and A.V. Kuznetsov, *AIP Conference Proceedings*, **2053**: 020003 (2018); https://doi.org/10.1063/1.5084349
13. A.N. Bol'shakova, I.Y. Efimochkin, and A.P. Bobrovskii, *Inorganic Materials: Applied Reserach*, **9**: 197–200 (2018); https://doi.org/10.1134/S2075113318020077
14. E.N. Kablov, *Aviations Materials and Tekhnologies*, **1**: 3–33 (2015); https://doi.org/10.18577/2071-9140-2015-0-1-3-33
15. N. Chawla and K.N. Chawla, *Metal Matrix Composites* (New York: Springer Science+Business Media: 2013).
16. M.F. Ashby and Y.J.M. Bréchet, *Acta Materialia*, **51**, No. 19: 5801–5821 (2003); https://doi.org/10.1016/S1359-6454(03)00441-5
17. R. Alderliesten, *Fatigue and Fracture of Fibre Metal Laminates* (Springer: 2017). https://doi.org/10.1007/978-3-319-56227-8
18. D. Brigante, *New Composite Materials: Selection, Design, and Application* (Springer: 2014); https://doi.org/10.1007/978-3-319-01637-5
19. R.M. German, *Particulate Composites: Fundamentals and Applications* (Springer: 2016), p. 363; https://doi.org/10.1007/978-3-319-29917-4_11
20. V.I. Kuz'min, V.I. Lysak, S.V. Kuz'min, and E.V. Kuz'min, *Composite Interfaces* **31**, No. 1: 1–24 (2023); https://doi.org/10.1080/09276440.2023.2248767
21. E.S. Karakozov, *Pressure Welding of Metals* (Moskva: Mashinostroenie: 1970) (in Russian).
22. M. Parks, *The Welding Journal*, **5**: 32 (1953).
23. M.Y. Brovman, *Russian Metallurgy (Metally)*, **2012**: 362–369 (2012); https://doi.org/10.1134/S0036029512050060
24. B.A. Greenberg, M.A. Ivanov, and V.V. Rybin, *Physics of Metals and Metallography*, **113**: 176–189 (2012); https://doi.org/10.1134/S0031918X12020056
25. I. Volokitina, A. Volokitin, E. Panin, T. Fedorova, D. Lawrinuk, A. Kolesnikov, A. Yerzhanov, Z. Gelmanova, and Y. Liseitsev, *Case Studies in Construction Materials*, **19**: e02609 (2023); https://doi.org/10.1016/j.cscm.2023.e02609

26. I. Volokitina, B. Sapargaliyeva, A. Agabekova, A. Volokitin, S. Syrlybekkyzy, A. Kolesnikov, G. Ulyeva, A. Yerzhanov, and P. Kozlov, *Case Studies in Construction Materials*, **18**: e02162 (2023); https://doi.org/10.1016/j.cscm.2023.e02162
27. I. Volokitina, *Journal of Chemical Technology and Metallurgy*, **57**, No. 3: 631–636 (2022).
28. I.E. Volokitina and A.V. Volokitin, *Metallurgist*, **67**: 232–239 (2023); https://doi.org/10.1007/s11015-023-01510-7
29. A.V. Volokitin, I.E. Volokitina, and E.A. Panin, *Progress in Physics of Metals*, **23**, No. 3: 411–437 (2022); https://doi.org/10.15407/ufm.23.03.411
30. A. Nurumgaliyev, T. Zhuniskaliyev, V. Shevko, and G. Yerekeyeva, *Scientific Reports*, **14**: 7456 (2024); https://doi.org/10.1038/s41598-024-57529-6
31. G. Kurapov, E. Orlova, and A. Turdaliev, *Journal of Chemical Technology and Metallurgy*, **51**, No. 4: 451–457 (2016).
32. S. Lezhnev and T. Koinov, *Journal of Chemical Technology and Metallurgy*, **49**, No. 6: 621–630 (2014).
33. Ya.S. Karpov and O.V. Ivanovskaya, *Composite Materials: Components, Structure, Processing into Products* (Kharkiv: National Aerospace University: 2001).
34. O.D. Sherby, J. Wadsworth, R.D. Caligiuri, and L.E. Eiisestein, *Scripta Metallurgica*, **13**: 941–946 (1979).
35. S. Kunda and M. Ghosh, *Material Science and Engineering: A*, **407**, Nos. 1–2: 154–160 (2005); https://doi.org/10.1016/j.msea.2005.07.010
36. N. Masahash and K. Komatsu, *Journal of Alloys and Compounds*, **379**, Nos. 1–2: 272–279 (2004); https://doi.org/10.1016/j.jallcom.2004.02.043
37. M. Talebian and M. Alizadeh, *Materials Science and Engineering: A*, **590**: 186–193 (2014); https://doi.org/10.1016/j.msea.2013.10.026
38. I. Itoh, K. Fujisawa, and H. Otsuka, *Nippon Steel Technical Report. Overseas*, **85**: 118–124 (2002).
39. B.A. Greenberg, M.A. Ivanov, A.V. Inozemtsev, M.S. Pushkin, A.M. Patselov, O.A. Elkina, S.V. Kuzmin, and V.I. Lysak, *Physics of Metals and Metallography*, **117**: 1219–1225 (2016); https://doi.org/10.1134/S0031918X16120073
40. A. Naizabekov, A. Arbuz, S. Lezhnev, E. Panin, and I. Volokitina, *Physica Scripta*, **94**, No. 10: 105702 (2019); https://doi.org/10.1088/1402-4896/ab1e6e
41. I.E. Volokitina and G.G. Kurapov, *Metal Science and Heat Treatment*, **59**, Nos. 11–12: 786–792 (2018); https://doi.org/10.1007/s11041-018-0227-0
42. A.B. Naizabekov, S.N. Lezhnev, and I.E. Volokitina, *Metal Science and Heat Treatment*, **57**, Nos. 5–6: 254–260 (2015); https://doi.org/10.1007/s11041-015-9870-x
43. I. Volokitina, B. Sapargaliyeva, A. Agabekova, S. Syrlybekkyzy, A. Volokitin, L. Nurshakhanova, F. Nurbaeva, A. Kolesnikov, G. Sabyrbayeva, A. Izbassar, O. Kolesnikova, Yu. Liseitsev, and S. Vavrenyuk, *Case Studies in Construction Materials*, **19**: e02256 (2023); https://doi.org/10.1016/j.cscm.2023.e02256

44. Q. Chu, M. Zhang, J. Li, and C. Yan, *Materials Science and Engineering: A*, **689**: 323–331 (2017).
45. I.A. Bataev, A.A. Bataev, V.I. Mali, and D.V. Pavliukova, *Material & Design*, **35**: 225–234 (2012); https://doi.org/10.1016/j.matdes.2011.09.030
46. I.A. Bataev, T.S. Ogneva, A.A. Bataev, V.I. Mali, M.A. Esikov, D.V. Lazurenko, Y. Guo, and A.M. Jorge Junior, *Materials & Design*, **88**: 1082–1087 (2015); https://doi.org/10.1016/j.matdes.2015.09.103
47. V.I. Mali, A.A. Bataev, I.N. Maliutina, V.D. Kurguzov, I.A. Bataev, M.A. Esikov, and V.S. Lozhkin, *The International Journal of Advanced Manufacturing Technology*, **93**: 4285–4294 (2017); https://doi.org/10.1007/s00170-017-0887-8
48. M. Konieczny, *Materials Characterization*, **70**: 117–124 (2012); https://doi.org/10.1016/j.matchar.2012.05.007
49. S.V. Smirnov and I.A. Veretennikova, *Diagnostics, Resource and Mechanics of Materials and Structures*, **4**: 6–15 (2015); https://doi.org/10.17804/2410-9908.2015.4.006-017
50. S. Lezhnev and A. Naizabekov, *Journal of Chemical Technology and Metallurgy*, **52**, No. 4: 626 (2017).
51. S.N. Lezhnev, I.E. Volokitina, and A.V. Volokitin, *Physics of Metals and Metallography*, **118**, No. 11: 1167–1170 (2017); https://doi.org/10.1134/S0031918X17110072
52. S. Lezhnev, E. Panin, and I. Volokitina, *Advanced Materials Research*, **814**: 68–75 (2013); https://doi.org/10.4028/www.scientific.net/AMR.814.68
53. A.V. Volokitin, M.A. Latypova, A.T. Turdaliev, and O.G. Kolesnikova, *Progress in Physics of Metals*, **24**, No. 4: 686–714 (2023); https://doi.org/10.15407/ufm.24.04.686
54. A.T. Turdaliev, M.A. Latypova, and E.N. Reshotkina, *Progress in Physics of Metals*, **24**, No. 4: 792–818 (2023); https://doi.org/10.15407/ufm.24.04.792
55. A. Volokitin, A. Naizabekov, I. Volokitina, and A. Kolesnikov, *Journal of Chemical Technology and Metallurgy*, **57**: 809 (2022).
56. A. Mozaffari, H. Danesh Manesh, and K. Janghorban, *Journal of Alloys and Compounds*, **489**, No. 1: 103–109 (2010); https://doi.org/10.1016/j.jallcom.2009.09.022
57. H. Sieber, J.S. Park, J. Weissmuller, and J.H. Perepezko, *Acta Materialia*, **49**: 1139–1151 (2001); https://doi.org/10.1016/S1359-6454(01)00023-4
58. Y. Saito, H. Utsunomiya, N. Tsuji, and T. Sakai, *Acta Materialia*, **47**: 579–583 (1999); https://doi.org/10.1016/S1359-6454(98)00365-6
59. N. Kamikawa, N. Tsuji, and Y. Minamino, *Science and Technology of Advanced Materials*, **5**: 163–172 (2004); https://doi.org/10.1016/j.stam.2003.10.018
60. M. Alizadeh, M. Ghaffari, H. Akbari beni, and R. Amini, *Materials and Design*, **50**: 427–432 (2013); https://doi.org/10.1016/j.matdes.2013.03.018
61. M. Alizadeh and M. Paydar, *Materials Science and Engineering: A*, **538**: 14–19 (2012); http://doi.org/10.1016/j.msea.2011.12.101

62. M. Alizadeh, *Materials Letters*, **64**: 2641–2643 (2010); https://doi.org/10.1016/j.matlet.2010.08.039
63. R. Vintila, A. Charest, R.A.L. Drew, and M. Brochu, *Materials Science and Engineering: A*, **528**: 4395–4407 (2011); https://doi.org/10.1016/j.msea.2011.02.079
64. Z. Mo, Y. Liu, J. Geng, and T. Wang, *Materials Science and Engineering: A*, **652**: 305–314 (2016); https://doi.org/10.1016/j.msea.2015.11.089
65. I.J. Beyerlein, N.A. Mara, J.S. Carpenter, and T. Nizolek, *Journal of Materials Reserarch*, **28**: 1799–1812 (2013); https://doi.org/10.1557/jmr.2013.21
66. E.H. Ekiz, T.G. Lach, R.S. Averback, N.A. Mara, I.J. Beyerlein, M. Pouryazdan, and P. Bellon, *Acta Materialia*, **72**: 178–191 (2014); https://doi.org/10.1016/j.actamat.2014.03.040
67. L. Ghalandari, M.M. Mahdavian, and M. Reihanian, *Materials Science and Engineering: A*, **593**: 145–152 (2014); https://doi.org/10.1016/j.msea.2013.11.026
68. L. Ghalandari and M.M. Moshksar, *Journal of Alloys and Compounds*, **506**: 172–178 (2010); https://doi.org/10.1016/j.jallcom.2010.06.172
69. P.H. Shingu, K. Yasuna, K.N. Ishihara, A. Otsuki, and M. Terauchi, *Materials Science Forum*, **235–238**: 35–40 (1997); https://doi.org/10.4028/www.scientific.net/MSF.235-238.35
70. B. Huang, K.N. Ishihara, and P.H. Shingu, *Journal of Materials Science Letters*, **20**: 1669–1670 (2001); https://doi.org/10.1023/A:1012465117652
71. R.D. Price, F. Jiang, R. Kulin, and K. Vecchio, *Materials Science and Engineering: A*, **528**: 3134–3146 (2011). https://doi.org/10.1016/J.MSEA.2010.12.087
72. I.E. Volokitina and A.V. Volokitin, *Physics of Metals and Metallography*, **119**, No. 9: 917–921 (2018); https://doi.org/10.1134/S0031918X18090132
73. I.E. Volokitina, *Metal Science and Heat Treatment*, **61**: 234–238 (2019); https://doi.org/10.1007/s11041-019-00406-1
74. I.E. Volokitina, *Metal Science and Heat Treatment*, **62**: 253–258 (2020); https://doi.org/10.1007/s11041-020-00544-x
75. S. Lezhnev, A. Naizabekov, E. Panin, and I. Volokitina, *Procedia Engineering*, **81**: 1499–1504 (2014); https://doi.org/10.1016/j.proeng.2014.10.180
76. S. Lezhnev and A. Naizabekov, *Procedia Engineering*, **81**: 1505 (2014); https://doi.org/10.1016/j.proeng.2014.10.181
77. G.R. Cowan, O.R. Bergmann, and A.H. Holtzman, *Metallurgical and Materials Transactions B*, **2**, No. 11: 3145–3155 (1971); https://doi.org/10.1007/bf02814967
78. D.V. Lazurenko, I.A. Bataev, V.I. Mali, E.A. Lozhkina, M.A. Esikov, and V.A. Bataev, *Physics of Metals and Metallograpgy*, **119**: 469–476 (2018); https://doi.org/10.1134/S0031918X18050095
79. I.A. Bataev, A. Bataev, V.I. Mali, M.A. Esikov, and V.A. Bataev, *Materials Science Forum*, **673**: 95–100 (2011); https://doi.org/10.4028/www.scientific.net/MSF.673.95
80. N. Tsuji, Y. Saito, S.H. Lee, and Y. Minamino, *Advanced Engineering Materials*, **5**: 338–344 (2003);

https://doi.org/10.1002/adem.200310077
81. X. Huang, N. Tsuji, N. Hansen, and Y. Minamino, *Materials Science and Engineering: A*, **340**: 265–271 (2003);
https://doi.org/10.1016/S0921-5093(02)00182-X
82. H. Akbari M. Alizade, M. Ghaffari, and R. Amini, *Composites Part B: Engineering*, **58**: 438–442 (2014);
https://doi.org/10.1016/j.compositesb.2013.10.037
83. H.S. Chen, W.X. Wang, Y.S. Li, P. Zhang, H.H. Nie, and Q.C. Wu, *Journal of Alloys and Compounds*, **632**: 23–29 (2015);
https://doi.org/10.1016/j.jallcom.2015.01.048
84. A.S. Smirnov, A.V. Konovalov, G.A. Belozerov, V.P. Shveikin, and E.O. Smirnova, *International Journal of Minerals, Metallurgy, and Materials*, **23**: 563–571 (2016);
https://doi.org/10.1007/s12613-016-1267-3
85. M.R. Toroghinejad, R. Jamaati, A. Nooryan, and H. Edris, *Ceramic International*, **40**: 10489–10498 (2014);
https://doi.org/10.1016/j.ceramint.2014.03.020
86. A. Volokitin, I. Volokitina, and E. Panin, *Metallography, Microstructure, and Analysis*, **13**: 1013–1016 (2024);
https://doi.org/10.1007/s13632-024-01078-x
87. I.E. Volokitina, A.I. Denissova, A.V. Volokitin, and E.A. Panin, *Progress in Physics of Metals*, **25**, No. 1: 132–160 (2024);
https://doi.org/10.15407/ufm.25.01.132
88. A.B. Nayzabekov and I.E. Volokitina, *Physics of Metals and Metallography*, **120**, No. 2: 177–183 (2019);
https://doi.org/10.1134/S0031918X19020133
89. D.A. Sinitsin, A.E. Elrefaei, A.O. Glazachev, E.I. Kayumova, and I.V. Nedoseko, *Construction Materials and Products*, **6**, No. 6: 2 (2023);
https://doi.org/10.58224/2618-7183-2023-6-6-2
90. I.E. Volokitina, A.I. Denissova, A.V. Volokitin, T.D. Fedorova, and D.N. Lavrinyuk, *Progress in Physics of Metals*, **25**, No. 1: 161–194 (2024);
https://doi.org/10.15407/ufm.25.01.161
91. I. Volokitina, N. Vasilyeva, R. Fediuk, and A. Kolesnikov, *Materials*, **15**, No. 11: 3975 (2022);
https://doi.org/10.3390/ma15113975
92. C. Lu, K. Tieu, and D. Wexler, *Journal of Materials Processing Technology*, **209**: 4830–4834 (2009);
https://doi.org/10.1016/j.jmatprotec.2009.01.003
93. A. Alizadeh, A. Abdollahi, and M.J. Radfar, *Transactions of Nonferrous Metals Society of China*, **27**, No. 6: 1233–1247 (2017);
https://doi.org/10.1016/S1003-6326(17)60144-4
94. J.D. Embury, N.J. Petch, and A.E. Wraith, *Transaction of Metal Science*, **239**: 114–118 (1967).
95. M. Pozuelo, F. Carreno, and O.A. Ruano, *Composites Science and Technology*, **66**, No. 15: 2671–2676 (2006);
https://doi.org/10.1016/j.compscitech.2006.03.018
96. Z. Wadsworth and D.R. Lesuer, *Materials Characterization*, **45**: 289–313 (2000);
https://doi.org/10.1016/S1044-5803(00)00077-2
97. D.W. Kum, T. Oyama, J. Wadsworth, and O.D. Sherby, *Journal of the Mechanics and Physics of Solids*, **31**: 173–186 (1983);
https://doi.org/10.1016/0022-5096(83)90049-2

98. P. Szroeder, I. Sahalianov, T. Radchenko, V. Tatarenko, and Yu. Prylutskyy, *Optical Materials*, **96**: 109284 (2019); https://doi.org/10.1016/j.optmat.2019.109284
99. T.M. Radchenko, V.A. Tatarenko, and G. Cuniberti, *Materials Today: Proceedings*, **35**, Pt. 4: 523–529 (2021); https://doi.org/10.1016/j.matpr.2019.10.014
100. T.M. Radchenko, I.Yu. Sahalianov, V.A. Tatarenko, Yu.I. Prylutskyy, P. Szroeder, M. Kempiński, and W. Kempiński, *Springer Proceedings in Physics: Nanooptics, Nanophotonics, Nanostructures, and Their Applications* (Eds. O. Fesenko and L. Yatsenko) (Springer, Cham: 2018), Vol. **210**, Ch. 3, p. 25–41; https://doi.org/10.1007/978-3-319-91083-3_3
101. I.Yu. Sahalianov, T.M. Radchenko, V.A. Tatarenko, and Yu.I. Prylutskyy, *Annals of Physics*, **398**: 80–93 (2018); https://doi.org/10.1016/j.aop.2018.09.004
102. I.Yu. Sagalianov, T.M. Radchenko, V.A. Tatarenko, and G. Cuniberti, *EPL (Europhysics Letters)*, **132**: 48002 (2020); https://doi.org/10.1209/0295-5075/132/48002
103. O.S. Skakunova, S.I. Olikhovskii, T.M. Radchenko, S.V. Lizunova, T.P. Vladimirova, and V.V. Lizunov, *Scientific Reports*, **13**: 15950 (2023); https://doi.org/10.1038/s41598-023-43269-6
104. D.M.A. Mackenzie, M. Galbiati, X.D. de Cerio, I.Y. Sahalianov, T.M. Radchenko, J. Sun, D. Peña, L. Gammelgaard, B.S. Jessen, J.D. Thomsen, P. Bøggild, A. Garcia-Lekue, L. Camilli, and J.M. Caridad, *2D Materials*, **8**, No. 4: 045035 (2021); https://doi.org/10.1088/2053-1583/ac28ab
105. T.M. Radchenko, A.A. Shylau, and I.V. Zozoulenko, *Physical Review B*, **86**, No. 3: 035418 (2012); https://doi.org/10.1103/PhysRevB.86.035418
106. T.M. Radchenko, A.A. Shylau, I.V. Zozoulenko, and A. Ferreira, *Physical Review B*, **87**, No. 19: 195448 (2013); https://doi.org/10.1103/PhysRevB.87.195448
107. T.M. Radchenko, A.A. Shylau, and I.V. Zozoulenko, *Solid State Communications*, **195**: 88–94 (2014); https://doi.org/10.1016/j.ssc.2014.07.012
108. S.P. Repetsky, I.G. Vyshyvana, S.P. Kruchinin, V.B. Molodkin, and V.V. Lizunov, *Metallofizika i Noveishie Tekhnologii*, **39**, No. 8: 1017–1022 (2017); https://doi.org/10.15407/mfint.39.08.1017
109. R. Balabai, A. Solomenko, and D. Kravtsova, *Molecular Crystals and Liquid Crystals*, **673**, No. 1: 125–136 (2018); https://doi.org/10.1080/15421406.2019.1578502
110. R.M. Balabai and A.G. Solomenko, *Journal of Nano- and Electronic Physics*, **11**, No. 5: 05033 (2019); https://doi.org/10.21272/jnep.11(5).05033
111. A.G. Solomenko, I.Y. Sahalianov, T.M. Radchenko, and V.A. Tatarenko, *Molecular Crystals and Liquid Crystals*, **768**, No. 9: 238–250 (2024); https://doi.org/10.1080/15421406.2024.2348204
112. A.G. Solomenko, I.Y. Sahalianov, T.M. Radchenko, and V.A. Tatarenko, *Scientific Reports*, **13**: 13444 (2023); https://doi.org/10.1038/s41598-023-40541-7
113. R.L. Woodward, S.R. Tracey, and I.G. Crouch, *Journal of Physique IV*, **1**: 277–282 (1991).

Received 23.06.2024
Final version 05.11.2024

*М.А. Латипова, Б.Б. Махмутов, А.С. Єржанов*
Караґандинський індустріальний університет,
просп. Республіки, 30, 101400 Темиртау, Казахстан

## ШАРУВАТІ МЕТАЛЕВІ КОМПОЗИТИ ЯК ПЕРСПЕКТИВНИЙ КЛАС СУЧАСНИХ МАТЕРІАЛІВ

Інтенсивний розвиток транспортного, хімічного, атомно-енергетичного машинобудування, суднобудування й авіакосмічної техніки зумовлює необхідність створення нових матеріалів, що мають унікальний набір фізико-механічних і функціональних властивостей. До таких матеріалів належить широка група шаруватих металевих композитів на основі різноманітних металів і сплавів, які завдяки наявності ламінованої та сандвічевої структур дають змогу одержати комплекс властивостей, що важко поєднуються: високу міцність, пластичність, ударну в'язкість за низьких кліматичних і кріогенних температур, зносостійкість, тепло- й електропровідність. Одним з актуальних напрямів сучасного матеріалознавства є розроблення шаруватих металевих композиційних матеріалів багатофункціонального призначення з шарами із консолідованих сумішей порошків Al та зміцнювальних частинок $Al_2O_3$, SiC і $B_4C$, які можуть використовуватися для виготовлення виробів і конструкцій із заданими трибологічними та теплофізичними характеристиками, високою балістичною стійкістю, а також для виробництва радіаційно-захисних елементів атомної чи то космічної техніки.

**Ключові слова:** шаруваті матеріали, композиційні матеріали, структура, властивості, методи виробництва.